Understanding the Development of Motion Processing by Characterizing Optic Flow Experienced by Infants and their Mothers

F. Raudies, R.O. Gilmore, K.S. Kretch, J.M. Franchak, and K.E. Adolph

Abstract— **Understanding the development of mature motion processing may require knowledge about the statistics of the visual input that infants are exposed to, how these change across development, and how they influence the maturation of motion-sensitive brain networks. Here we develop a set of techniques to study the optic flow experienced by infants and mothers during locomotion as a first step toward a broader analysis of the statistics of the natural visual environment during development.**

Index Terms— **Optic flow, self-motion, eye-tracking, gaze, heading.**

I. WHAT DOES OPTIC FLOW TELL US ABOUT HUMAN BEHAVIOR?

OPTIC flow, the pattern of motion generated by observer movement, specifies the direction and speed of progression through the environment [1]. Different observer motions generate distinctive optic flow patterns. Forward translation generates a radially expanding pattern containing a vanishing point called the focus of expansion (FOE) that specifies the observer's instantaneous direction of motion. Additionally, rotations around the gaze axis produce a center of rotation (COR) around which flow vectors orbit. Natural behavior consists of a mixture of eye rotations, head translations and rotations, and body translations and rotations. Thus, the pattern of optic flow experienced by human observers in natural environments is a complex mixture that to our knowledge has not previously been characterized.

Behavioral sensitivity to optic flow in humans and non-human primates [2] emerges early, but develops slowly [3-6]. Development may stem from changes in neural substrates such as cortical areas MT or MST that appear selective for complex motion patterns [7-9]. We hypothesize that development in neural circuitry may be shaped by changes in the statistics of the visual input. Observers experience different patterns of flow when lying down, being carried, sitting upright, crawling, or walking. As a result of developmental changes in posture and locomotion [10,11], the optic flow patterns experienced across development must also undergo substantial change.

Here, we demonstrate techniques to describe the statistics of optic flow during natural behavior using a combination of head-mounted eye-tracking and computer vision methods. As a starting point for a more comprehensive analysis, we analyze the optic flow patterns experienced by infants and adults— specifically, mothers carrying their infants in an indoor environment. Because the environment is identical and mothers control the speed and direction of body movement, we predict that flow patterns will be maximally similar under these conditions. We ask: What kinds of flow patterns do infants and adults experience? How often are particular flow patterns experienced? How are the statistics of flow similar or different?

The answers serve several purposes. The data can provide input to computational models of the motion processing system and may have implications for the development of training regimes for autonomous agents or mobile robots. Moreover, the data can be used to make predictions about developmental patterns in behavioral sensitivity early emerging sensitivity to that can be tested using psychophysical [2] or psychophysiological [9] techniques. For example, young primates show stronger responses to fast linear flows. Might these biases reflect statistical regularities in the input?

F. Raudies is with the Boston University, Boston MA 02215 USA (phone: 617-435-7918; e-mail: fraudies@bu.edu).
R.O. Gilmore is with Penn State University, University Park, PA 16802 USA (e-mail: rogilmore@psu.edu).
K.S. Kretch is with New York University, New York, NY 10013 USA (e-mail: ksk288@nyu.edu).
J.M. Franchak is with New York University, New York, NY 10013 USA (e-mail: franchak@gmail.com)
K.E. Adolph is with New York University, New York, NY 10013 USA (e-mail: karen.adolph@nyu.edu)

II. ESTIMATION OF OPTIC FLOW AND SELF-MOTION FROM VIDEO

Data for optic flow analysis were collected using two Positive Science head-mounted eye-trackers [12,13]. Six 9.5-month-old infants rode in a forward-facing infant carrier as their mothers walked around the hallways of an academic building. Both infants and mothers wore the head-mounted eye trackers, each of which consisted of two miniature cameras. The eye camera recorded participants' eye movements and the scene camera, positioned above the right eye, recorded a head-centered field of view. Scene cameras

(3.6 × 2.7 mm, focal length of 3.5 mm) provided a visual field of view of 54.4° × 42.2° and recorded videos at a resolution of 640 × 480 pixels at 30 Hz. A calibration procedure yielded xy-coordinates of infants' and mothers' point of gaze with a spatial accuracy of 2°. We selected sequences of about 30 sec (≈900 frames) that excluded independently moving objects. Dyads made a single pass through the same hallway.

Optic flow was estimated from the scene camera videos. First, we describe the method that we use to estimate optic flow from videos. Second, we describe a set of biologically plausible flow patterns that we use to characterize the camera flow of infants and mothers. Third, we describe two methods that estimate self-motion from optic flow.

We assume constant grayscale values for the estimation of optic flow. From one video frame to the next, grayscale values change only due to a spatial shift; otherwise their values stay constant. A violation of this constraint occurs if light is dimmed. Grayscale constancy is not sufficient to constrain the solution space for possible optic flows in a video signal. Thus, flow estimation incorporates additional constraints, e.g., the smoothness constraint. Smoothness of flow assumes coherent motion of rigid objects: Neighboring points in the image plane are likely to move together. At discontinuities in the flow, the smoothness constraint should not apply. Such discontinuities are the boundary of objects that appear in different depths or at the boundary of objects that move differently. Reference [14] proposes a smoothness constraint based on the norm of the partial derivative of optic flow. This constraint has been refined by [15] introducing the non-linear penalizing function and assuming constancy of the gray-value gradients—in terms of lightness changes in the video—in addition to grayscale constancy. The functional that combines all three constraints is:

$$E(u,v) = \int_{\Omega_{\bar{x}}} \psi\left(\left|g(\bar{x}+\bar{w})-g(\bar{x})\right|^2 + \gamma \cdot \left|\nabla g(\bar{x}+\bar{w})-\nabla g(\bar{x})\right|^2\right)$$
$$+ \alpha \cdot \psi\left(\left|\nabla u\right|^2 + \left|\nabla v\right|^2\right) d\bar{x} \tag{1}$$

with the grayscale value function g and the parameters α, γ, and ε. The vector $\bar{x} = (x,y,t)$ denotes a location in the image plane. The vector $\bar{w} = (u,v,\Delta)$ denotes the warping vector, where the image frame from time $t+\Delta$ is warped backward to match the image frame at time t. An error-free match gives $g(\bar{x}+\bar{w}) = g(\bar{x})$. In reality, an error-free match is typically not achieved due to noise and discretization errors. Thus, (1) is minimized with respect to the unknowns u and v, using the Euler Lagrange equations. The resulting minimization yields two non-linear, coupled partial differential equation systems (PDEs). A numerical discretization and fix-point iteration to address non-linearity results in a sparse linear equation system that we solve using the method of Successive Over-Relaxation (SOR). See more details in [16] on page 84ff. We use the described numerical method to solve (1) and, thus, compute the optic flow u and v from a video that defines the gray-value function g.

Next, we describe how the detected scene camera flow is mapped into a set of biologically inspired flow patterns to characterize the experienced flow in biologically plausible way. We pre-define flow patterns and their detection from

estimated optic flow based on neurophysiological findings about sensitivity in the medial superior temporal (MST) area of the primate cerebral cortex [7,8]. Sensitivity is described for a pattern of expansion flow with the focus of expansion (FOE) shifted in the image plane. Such patterns are generated by forward motion of the observer; the shift of the FOE is a result of the combination of forward motion with sideward or up/downward motion. Other cells in MST are sensitive to laminar motion in various directions in the image plane, e.g. leftward, rightward, upward, or downward. Yet another cell type is sensitive to curl patterns of flow that are a result of rotations around the optical axis. This flow pattern has a center of rotation (COR) aligned with the center of the image plane. Neurons show selectivity to flow patterns with a shifted COR that are not aligned with the center of the image plane. This shift can be produced by a superposition of roll with yaw (vertical axis) and or pitch (horizontal axis) rotation. In our model we denote the linear velocity along the optical axis by v_z and the rotation around the optical axis by ω_z. Shifts of the FOE or COR are denoted by x_0 and y_0. Laminar flow patterns are defined by the angle φ and the speed v_l. The expected pattern of flow for these parameters is:

$$\begin{pmatrix} \dot{x} \\ \dot{y} \end{pmatrix} = \begin{pmatrix} x-x_0 \\ y-y_0 \end{pmatrix} \cdot v_z + \begin{pmatrix} \cos(\varphi) \\ \sin(\varphi) \end{pmatrix} \cdot v_l + \begin{pmatrix} +(y-y_0) \\ -(x-x_0) \end{pmatrix} \cdot \omega_z \tag{2}$$

For our model flow patterns, we chose $v_z = f/\sqrt{(x_0^2+y_0^2+f^2)}$ and $x_0 = \pm w/2$ or $x_0 = 0$ with $y_0 = \pm h/2$ or $y_0 = 0$ and $\omega_z = 1\,$rad/frame with w and h denoting the width and height of the image plane. Note that we either set v_z or v_l or ω_z to their described value, while setting the remaining variables to zero. The parameter φ is sampled between 0° and 340° in equal steps of 20°. This gives 18 patterns for each of the three categories, or in total 54 flow patterns. All these patterns are matched to the flow input $(\dot{x}, \dot{y})$ that is computed by solving (1). A match is computed in two steps. First, we compute the inner product between flow input and flow pattern:

$$m_{\cos}(v_z, v_l, \omega_z, x_0, y_0, \varphi) = \frac{\dot{\hat{x}} \cdot \dot{x} + \dot{\hat{y}} \cdot \dot{y}}{\sqrt{\dot{\hat{x}}^2 + \dot{\hat{y}}^2} \cdot \sqrt{\dot{x}^2 + \dot{y}^2}} \tag{3}$$

This match m_{cos} in (3) computes a cosine tuning between the flow input and flow pattern. In the notation of (3) we dropped the dependency of the pattern flow on all variables. The second step of our detector implements inhibition between antagonistic flow patterns. For instance, expansion is antagonistic to contraction. This second step computes

$$m_{ant}(v_z, v_l, \omega_z, x_0, y_0, \varphi) = \left[\frac{m_{\cos}^+ - m_{\cos}^-}{2 + m_{\cos}^+ + m_{\cos}^-}\right]^+ \tag{4}$$

where m_{cos}^+ denotes, e.g. expansion, and m_{cos}^- denotes, e.g. contraction. The value '2' in the denominator is caused by a shift of the cosine-tuning from the interval [-1, +1] to [0, 2]. Matches m_{ant} model neural responses to flow patterns for cells found in area MST. Next, we describe a more detailed method of extracting self-motion parameters from estimated optic flow.

We use optic flow to estimate the translational and rotational self-motion of the camera with respect to its orientation in 3D. For this estimation, we assume a pinhole camera model that has a high sampling rate and, thus, only small shifts and rotations between appear between two image

frames. Given these two criteria, we assume a differential motion model that expresses the image velocities $(u,v) = (\dot{x}, \dot{y})$ in terms of the 3D translational velocity (v_x, v_y, v_z) and 3D rotational velocities $(\omega_x, \omega_y, \omega_z)$. Reference [17] introduced the model for optic flow:

$$\begin{pmatrix} \dot{x} \\ \dot{y} \end{pmatrix} = \frac{1}{Z}\begin{pmatrix} -f & 0 & x \\ 0 & -f & y \end{pmatrix}\begin{pmatrix} v_x \\ v_y \\ v_z \end{pmatrix} + \frac{1}{f}\begin{pmatrix} x \cdot y & -(f^2 + x^2) & f \cdot y \\ (f^2 + y^2) & -x \cdot y & -f \cdot x \end{pmatrix}\begin{pmatrix} \omega_x \\ \omega_y \\ \omega_z \end{pmatrix} \quad (5)$$

This expression includes the focal length f of the pinhole camera, the image coordinates x and y, the distance Z of sample points measured along the optical axis of the pinhole camera, and the already described parameters for self-motion. In (5), the vector $(\dot{x}, \dot{y})$ is estimated from video. The vectors (v_x, v_y, v_z), $(\omega_x, \omega_y, \omega_z)$, and Z are unknowns. A linear-least squares optimization with squared distance norm using discretized flow results in a non-linear optimization problem, due to the product between the $1/Z$ and the linear velocity components v_x, v_y, and v_z. Two solutions exist that re-formulate the optimization to be a linear problem. Reference [18] transforms the flow Equation (5) into a subspace of constraints which depend only on the linear-velocities. This allows them to analytically estimate self-motion from optic flow. Reference [19] optimizes for Z first in order to derive a bilinear constraint, like in [20], and then introduces auxiliary variables that are products of linear and rotational velocities. This again results in a linear optimization problem with respect to the newly introduced auxiliary variables. We use these two methods to estimate self-motion because they do not require any numerical optimization. Instead, these methods compute an analytical solution for the chosen norm and space of optimization.

Rather than estimating self-motion based on optic flow from each pixel, we apply a confidence measure to make the dense flow data sparse. We use (1) as a measure of confidence in the estimated optic flow. Data from the video sequence is entered into (1) as g and estimated flow as u and v. Equation (1) provides a distance metric. We define its reciprocal as a measure of confidence. In our case, we made the optic flow sparse by taking the top 1% of the flow estimates with highest confidence values. This leaves us 3,072 data points per image frame. In theory, the estimation of self-motion requires at least five data points to uniquely constrain the solution. For reasons of noise and linear dependency in sample flow, we choose the one percent value or 3,072 data points increasing the signal-to-noise ratio (assuming noise being uncorrelated) and likelihood of sampling linearly independent.

III. Analyzing Video and Eye-Tracking Data from Infants and Mothers

There are many ways one might characterize the statistics of experienced optic flow and its relationship to gaze. Here, we illustrate a few analyses that show the potential power of the approach.

A. Infants experience faster image speeds than mothers

We computed optic flow for the six dyads and evaluated the distribution of pixel velocities across the entire image sequence for each dyad. Figure 1a-c shows examples of single
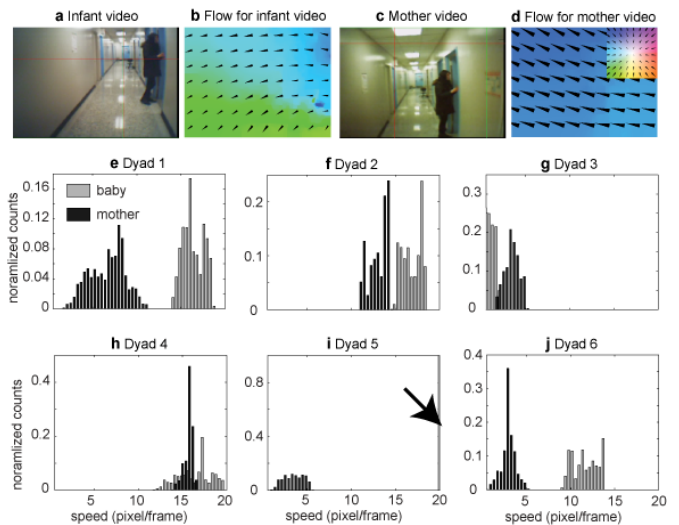

Fig. 1. **In most cases the pixel speed for infants is higher than that for mothers. a)** Video frame and **b)** estimated optic flow for an infant video. **c)** Video frame and **d)** estimated optic flow for the corresponding mother video. **e-j)** show histograms of pixel speeds from the entire video for each dyad.

video frames and the estimated optic flow field. We analyzed pixel velocities within a circular aperture that has a diameter equal to the smaller of the two image dimensions—this selection avoids a sample bias toward horizontal or vertical flows that would be introduced by pooling from a rectangular or squared image region. Each histogram in Figure 1e-j summarizes speeds of each pixel within the circular aperture across all video frames. In five out of six cases the distribution of pixel velocities for infants peaks at higher velocities than the distribution for mothers, with the exception of dyad 3 (Figure 1g). This shift toward higher pixel speeds could be explained by stronger head rotations (pitch) by infants compared to mothers, or by infants orienting their heads closer toward the ground than mothers. Further analyses below confirm both explanations.

B. Similar flow patterns are experienced by infants and mothers

Figure 2a-2c shows patterns of optic flow that are generated by self-motion. Radial flow patterns in Figure 2a are caused by translational self-motion in a forward/backward direction. Laminar patterns in Figure 2b are caused by translational self-motion parallel to the image plane of the pinhole camera (Equation 1 with $v_z = 0$) in a sideways or up/downward direction. Curl patterns are introduced by rotational self-motion $(\omega_x, \omega_y, \omega_z)$. Our operator that detects these patterns of flow is invariant with respect to the focus of expansion (FOE) in radial flow patterns, the direction of motion in laminar flow patterns, and the center of rotation (COR) in curl flow patterns. This invariance is achieved by computing the maximum response pattern for different positions of the FOE or COR, and different motion directions in the case of laminar flow. To increase the response strength, and simulate a form of direction tuning, our detector also computes an opponent response between expansion and contraction, upward laminar motion (0°-180°) and downward laminar motion (180°-360°),
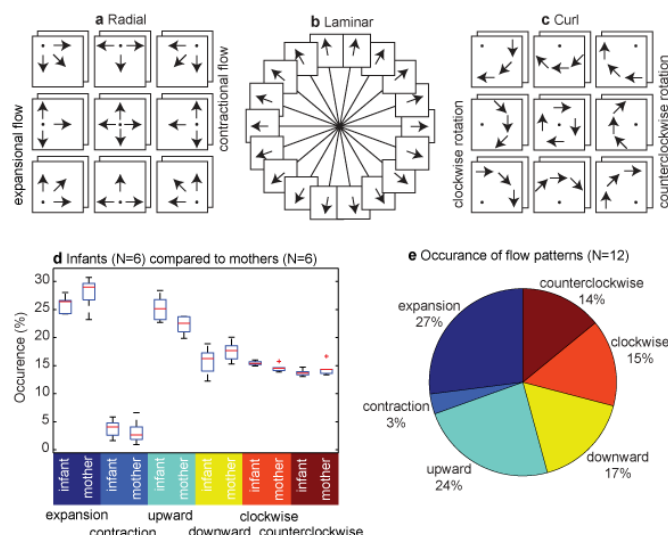
Fig. 2. **Flow patterns invariant to the FOE or COR experienced by infants and their mothers do not differ much.** a) Shows radial flow patterns that combined together, e.g. by selecting the maximum, are invariant to the FOE. Such patterns are generated by translational self-motion. b) Shows laminar flow patterns. All patterns combined are invariant to the direction of motion. c) Illustrates curl flow patterns and together these patterns are invariant to the COR. d) Compares the occurrence of flow patterns between infants and mothers. e) The overall occurrence of patterns from infants and mothers combined.

Fig. 3. **Responses of flow patterns suggest that mothers have a gait cycle of ≈1.5Hz.** a) Distribution of frequencies for laminar flow for infant and mother videos. b) "Best" case and c) "worst" case of the detected frequency.

or clockwise rotation and counterclockwise rotation. We measure the relative occurrence of these pattern responses—radial, laminar, or curl—with respect to the overall response of patterns in all frames. For instance, if all pattern detectors respond equally, their relative occurrence would be 8.33% because there are 12 patterns in total. Figure 2d shows the extracted response characteristic for infants and mothers. Infants and mothers showed similar distributions of flow patterns, so we combined the responses from infants and mothers to report the overall relative occurrence of flow patterns (Figure 2e). Expansion occurred most often (27%), followed by upward laminar motion (24%) and downward laminar motion (17%), and clockwise (15%) and counterclockwise (14%) rotation. Contraction had the lowest relative response (3%). More upward than downward motion responses provide an indicator that the camera/head is pointing toward the ground, and even more so for infants than for mothers (compare the upward/downward responses for infants and mothers in Figure 2d).

C. Flow patterns show the frequency of mothers' gait cycle

We examined the flow patterns to determine whether they contained a temporal structure. First, we removed any linear trend from each sequence by individual and pattern response. Second, we computed the Fourier transform and power for each sequence. Based on visual inspection, we assumed the frequency for which maximum power occurs was meaningful if the power (in arbitrary units) exceeded 0.3 and the frequency was larger than 0.1 Hz. This was the case for five infant sequences and four mother sequences. Figure 3a shows the distribution of the computed frequencies. The spread of
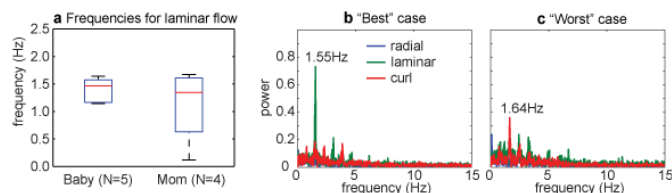
frequencies was wide, and more so for mothers than for infants. This suggests that mothers compensate better for the oscillatory motions associated with gait than the passively carried infants do. Or, alternatively, it suggests that the underlying oscillation might be amplified by infants' heads as a result of being carried. Figure 3b and 3c show spectra of our "best" and "worst" cases. This provides a motivation for the applied thresholds and shows that the oscillatory behavior can be discerned by looking at the spectra of laminar flow, the green curve in Figure 3b and 3c (note that in 3c the green curve appears behind the red curve).

D. Infants and mothers show important differences in location of the focus of expansion, direction of rotation, and direction of gaze

We estimated the direction of translational and rotational self-motion from optic flow using two methods [18,19]. The focus of expansion (FOE) specifies the direction of translation; the center of rotation (COR) specifies the axis of rotation. We evaluated only frames for which both algorithms estimated the FOE or COR within a difference of 2°. In the mean over all twelve videos (6 dyads), this criterion was met by about half of all image frames—about 4,500 frames in total—which was enough for our analysis. We computed the statistics of the FOE or COR direction with respect to the center of the image plane.

The statistics of infants' FOEs are shown in Figure 4a. Infants' FOE is biased towards the top of the visual field, which can be explained if infants' pointed their heads downward relative to the path of progression. Thus, with respect to the image plane of the scene camera worn by the infant, the linear velocity vector is pointing upward (also illustrated in Figure 4a). Figure 4b shows the COR statistics for infants; infants' CORs are spread around the horizontal axis. This means that infants experienced mainly a combination of roll and pitch head rotation. These pitch rotations are probably not voluntary, most likely they are imposed by the mother's gait. Figure 4c shows the statistics of the COF for infants. COFs are biased toward the lower-left due to the mounting point of the eye-tracker scene camera over the right eye.

Mothers' FOE data are shown in Figure 4d, which shows that the FOE is biased toward the upper half of the visual field, like infants, but also spread out to the left/right. This means that mothers' faces are tilted toward the ground and, in addition, explore the scene with more active leftward and rightward head rotations than infants do or are capable of given the physical constraints of the baby carrier. The
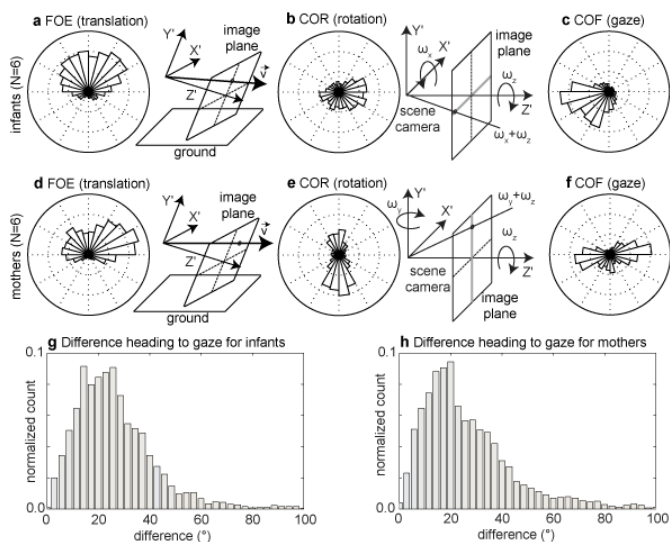
Fig. 4. **The FOE for infants is shifted upward, more so than for mothers. Infants experience imposed pitch rotation, mothers show explorative yaw rotations.** a-c) Direction of FOE, COR, and COF for infants. d-f) Same direction statistics for mothers. g) Angular difference between FOE and COF for infants and in h) for mothers.

statistics for the COR shown in Figure 4e confirm this. Rotations for mothers are a combination of roll and yaw. Figure 4f shows the COF statistics for mothers. This shows a leftward/rightward bias. Thus, mothers not only actively rotate their head left or right, but they also direct their gaze to the left and right.

E. Heading and gaze point in different directions for infants and mothers

Finally, we compared the estimated heading direction from the head-mounted camera (based on the position of the FOE in the image plane) to the gaze direction. All data references the image plane and orientation of the camera in 3D. In principle, it is possible to have a 180° difference in gaze and heading, if for example; the observer pointed her head toward the left and looked even further to the left while moving to the right. In our plots, the distance between heading and gaze ranged between 0° and 100°. Figures 4g and 4h show the data for infants and for mothers, respectively. Both distributions peak at ≈20°. Neither infants nor mothers spent considerable time looking where they were going. The results suggest that the direction of heading does not strongly attract infants' gaze under conditions of passive locomotion, nor adults' gaze under active locomotion, at least in these particular circumstances.

IV. DISCUSSION

Our data show that there are both similarities and differences in the statistics of optic flow that occur to both observers when mothers carry infants. Because this was a scenario in which we would expect infants and mothers to be maximally similar, the differences are interesting.

We found that most infants experienced faster flow speeds than their mothers. In our study this arises because infants point their head toward the ground while adults keep their heads more in a horizontal position, and infants experience frequent pitch rotations imposed by the mother's gait. These characteristics could be specific to the situation in which infants are carried in a forward facing carrier at chest height rather than carried in mothers' arms or pushed in a stroller. Whether the finding would generalize to other passive carrying situations or to active locomotion is not yet known. Nevertheless, both behavioral data with monkeys [2] and psychophysiological data with humans [9] show that infants are more sensitive to fast global motion patterns than slower ones. This suggests that the vision of infant primates may be tuned to dominant statistics of their experienced visual environments.

Researchers focused on infant development have begun to measure the experienced visual environment using head-mounted cameras [21-24] and eye-trackers [12,13] coupled with sophisticated video data analytic tools (http://openshapa.org). These techniques make it possible to answer a broad range of questions about the regularities in the natural environments experienced by human infants. Along these lines, our data and methods can provide insight into how developmental changes in the statistics of experienced optic flow may shape the development of motion processing.

These data from our analysis will provide input to a self-organizing computational model of the motion processing network we are now developing. The data also imply that subtle differences in the dynamics of sensory input may be important for other self-organizing – robotic or agent-based – systems.

Like any new technique, our approach has limitations. All participants walked down the same indoor hallway, but some dyads walked down the hallway when there were other people moving or doors opening. Independently moving objects generate patterns of optic flow that involve direction and speed gradients and shear edges. We omitted frames that contained these types of motion from analysis due to the challenge they provide to the estimation of self-motion from optic flow, and because existing solutions [25,26] have limitations. A detailed computational analysis of the problem is given by [27]. Another limitation concerned the modest spatial and temporal resolution of our measurements of both flow and gaze. When high-speed head or eye movements occurred, our flow estimation algorithm failed, and we lost data. On the other hand, higher resolution data streams would pose substantial additional computational demands. As it stands, our analysis pathway involved significant—hundreds of hours—of offline processing. Real-time or online processing of optic flow at 30 Hz with a resolution of 640 × 480 pixels is not possible with current general purpose hardware and software, although some methods [28,29] are close to computing pixel flow for a resolution of 640 × 480 pixels at 30 Hz.

A further limitation relates to our focus on optic flow generated by head movement. To compute flow patterns at the retina—the optimal measure of input to the optic flow processing system—would require us to combine flow from head movement with eye movement data, and then sample the estimated retinal flow fields. This poses difficult challenges

due to boundary effects, the size of the visual field sampled by the camera, and questions about how large a sample region is necessary to estimate retinal flow.

V. CONCLUSIONS

With data streams derived from head-mounted eye trackers and a rich image processing pipeline in place, it is possible to analyze the natural scene statistics of the visual environments experienced by infants, children and adults carrying out complex actions in natural environments. Thus, fundamental questions about the nature of visual experience and how it might change across development can now be asked in a systematic way. In the case of optic flow in passive locomotion, infants experience flows similar to adults, but there are subtle, potentially important differences in the overall speed of flow, the position and oscillation of the head, and the direction of gaze relative to the direction of self-motion. More precise measurements of the natural scene statistics for optic flow can provide additional constraints for self-organizing neural network models of the development of complex motion processing circuitry in the primate brain.

REFERENCES

[1] JJ. Gibson. The Ecological Approach to Visual Perception. Boston: Houghton-Mifflin, 1979.

[2] L. Kiorpes and J.A. Movshon. "Development of sensitivity to visual motion in macaque monkeys." Visual Neuroscience, vol. 21, 2004, pp. 851—859.

[3] O. Brosseau-Lachaine, C. Casanova, & J. Faubert. Infant Sensitivity to Radial Optic Flow Fields During the First Months of Life. Journal of Vision, vol. 8, no. 4, 2008.

[4] R.O. Gilmore, H.J. Rettke. Four-Month-Olds' Discrimination of Optic Flow Patterns Depicting Different Directions of Observer Motion, Infancy, vol. 4, no. 2, 2003, pp. 177—200.

[5] R.O. Gilmore, T.J. Baker, & K.H. Grobman. Stability in Young Infants' Discrimination of Optic Flow. Developmental Psychology, vol. 40, no. 2, 2004, pp. 259—270.

[6] J. Wattam-Bell, D. Birtles, P. Nyström, C. von Hofsten, K. Rosander, S. Anker, J. Atkinson, et al. Reorganization of Global Form and Motion Processing during Human Visual Development. Current Biology, vol. 20, no. 5, 2010, pp. 411—415.

[7] C. Duffy and R. Wurtz. "Response of monkey MST neurons to optic flow stimuli with shifted centers of motion." Journal of Neuroscience, vol. 15, no. 7, 1995, pp. 5192—5208.

[8] K. Tanaka, K. Hikosaka, H. Saito, M. Yukie, Y. Fukada, and E. Iwai. "Analysis of local and wide-field movements in the superior temporal visual areas of the macaque monkey." Journal of Neuroscience, vol. 6, no. 1, 1986, pp.134—144.

[9] C. Hou, R.O. Gilmore, M.W. Pettet, and A.M. Norcia. "Spatio-temporal tuning of coherent motion evoked responses in 4-6 month-old infants and adults." Vision Research, vol. 49, 2009, pp. 2509—2517.

[10] K.E. Adolph & S.E. Berger. Motor development. In W. Damon & R. Lerner (Series Eds.) & D. Kuhn & R. S. Siegler (Vol. Eds.), Handbook of child psychology: Vol. 2: Cognition, perception, and language (6th ed.) New York: Wiley, 2006, pp. 161—213.

[11] K.E. Adolph & S.R. Robinson (in press). The road to walking: What learning to walk tells us about development. In P. Zelazo (Ed.) Oxford handbook of developmental psychology. NY: Oxford University Press.

[12] J.M. Franchak, K. S. Kretch, K. C. Soska, J. S. Babcock, & K. E. Adolph. "Head-mounted eye-tracking of infants' natural interactions: a new method." Proceedings of the 2010 Symposium on Eye Tracking Research & Applications, Austin, Texas, 2010.

[13] J.M. Franchak, K.S. Kretch, K.C. Soska, and K.E. Adolph. "Head-mounted eye tracking: a new method to describe infant looking." Child Development, vol. 82, no. 6, 2011, pp. 1738—1750.

[14] B.K.P. Horn and B.G. Schunck. "Determining optic flow", Artificial Intelligence, vol. 17, 1981, pp. 185—203.

[15] T. Brox, A. Bruhn, N. Papenberg, and J. Weickert. "High accuracy optic flow estimation based on a theory of warping" In Proceedings of the 8th European Conference on Computer Vision, Springer LNCS 3024, T. Pajdla and J. Matas (Eds.), vol. 4, 2004, pp. 25—36.

[16] T. Brox. "From pixels to regions: partial differential equations in image analysis", PhD Thesis. Department of Mathematics and Computer Science Saarland University, 66041 Saarbrücken, Germany.

[17] H.C. Longuet-Higgins and K. Prazdny. "The interpretation of a moving retinal image". Proceedings of the Royal Society of London, Series B, Biology Sciences vol. 208, 1980, pp. 385—397.

[18] D.J. Heeger and A.D. Jepson. "Subspace methods for recovering rigid motion i: algorithm and implementation." International Journal of Computer Vision vol. 7, no. 2, 1992, 95—117.

[19] F. Raudies and H. Neumann. "An efficient linear method for the estimation of ego-motion from optical flow." In J. Denzler, G. Notni, and H. Süße (Eds.): DAGM 2009, LNCS 5748, 2009, pp. 11—20.

[20] A. Bruss and B. Horn. "Passive Navigation". Computer Vision, Graphics, and Image Processing, vol. 21, 1983, pp. 3—20.

[21] R.N. Aslin. How Infants View Natural Scenes Gathered From a Head-Mounted Camera. Optometry & Vision Science June 2009 vol. 86 no. 6, 2009, pp. 561—565.

[22] J.B. Cicchino, R.N. Aslin, & D.H. Rakison. Correspondences between what infants see and know about causal and self-propelled motion. Cognition, vol. 118 no. 2, 2011, pp. 171—192.

[23] L.B. Smith, C. Yu, & A.F. Pereira. Not your mother's view: the dynamics of toddler visual experience. Developmental Science, vol. 14, no. 1, 2011, pp. 9—17.

[24] C. Yu, T. Smith, S. Hidaka, M. Scheutz, & L. Smith. A Data-Driven Paradigm to Understand Multimodal Communication in Human-Human and Human-Robot Interaction. In P. Cohen, N. Adams, & M. Berthold (Eds.), Advances in Intelligent Data Analysis IX, Lecture Notes in Computer Science, Springer Berlin / Heidelberg, vol. 6065, 2010, pp. 232—244.

[25] W. MacLean, A. Jepson, and R. Frecker. "Recovery of egomotion and segmentation of independent object motion using the EM algorithm." In Proceedings of British Machine Vision Conference, vol. 1, 1994, pp.175—184.

[26] K. Pauwels and M. van Hulle. "Segmenting independently moving objects from egomotion flow fields." In Proceedings of the Early Cognitive Vision Workshop (ECOVISION 04), Isle of Skye, Scotland, 2004.

[27] F. Raudies and H. Neumann. "A review and evaluation of methods estimating ego-Motion." Computer Vision and Image Understanding vol. 116, 2012, pp. 606—633.

[28] A. Bruhn, J. Weickert, T. Kohlberger, C. Schnörr. "A multigrid platform for real-time motion computation with discontinuity-preserving variational methods." International Journal of Computer Vision, vol. 70, no. 3, 2006, pp. 257—277.

[29] C. Zach, T. Pock, and H. Bischof. "A duality based approach for real-time TV-L1 optical flow." In J. Denzler, G. Notni, and H. Süße (Eds.): DAGM 2009, LNCS 5748, 2009.